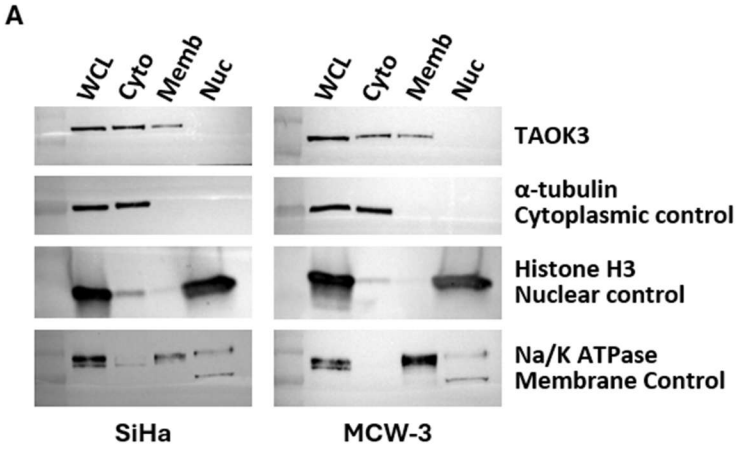

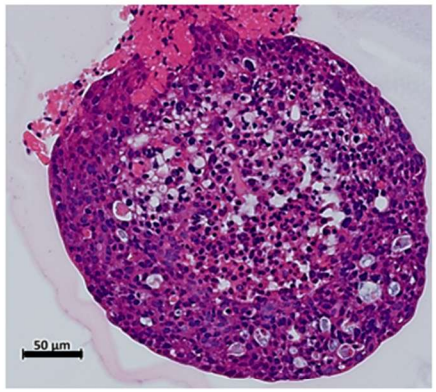

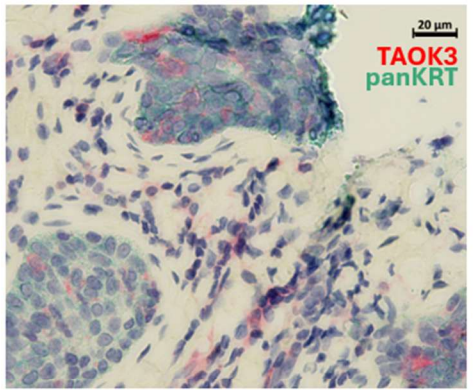

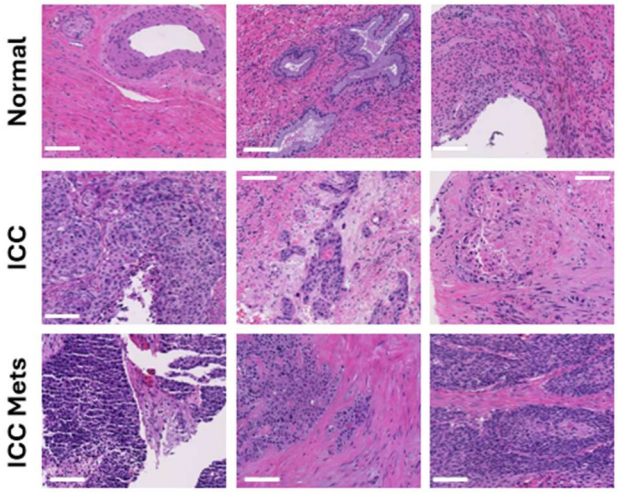

E

ID	Source	Term ID	Term Name	p_{adj} (query_1)
1	GO:MF	GO:0045296	cadherin binding	4.342×10^{-4}
2	GO:MF	GO:0044548	S100 protein binding	1.133×10^{-2}
3	GO:MF	GO:0004252	serine-type endopeptidase activity	4.854×10^{-2}
4	GO:BP	GO:0030855	epithelial cell differentiation	3.809×10^{-2}
5	GO:CC	GO:0005886	plasma membrane	1.559×10^{-5}
6	GO:CC	GO:0031982	vesicle	2.136×10^{-4}
7	GO:CC	GO:0030054	cell junction	2.859×10^{-3}
8	GO:CC	GO:0005829	cytosol	2.948×10^{-3}
9	GO:CC	GO:0031252	cell leading edge	4.637×10^{-2}

Supplementary Figure S1. *TAOK3* is expressed in a distinct subpopulation of cervical cancer epithelial cells. A, Western blotting of subcellular fractionations of SiHa and MCW-3 cervical cancer cells shows expression in whole cell lysate (WCL), cytoplasm (Cyto), and membrane (Memb), but not the nucleus (Nuc). **B,** H&E staining of cervical cancer patient-derived tumoroid used for TAOK3 IHC and HPV ISH. Scale bar (black) = 50 µm. **C,** Dual-color IHC of TAOK3 (red) and pan-keratin (green) in cervical cancer tumor tissue shows co-staining in tumor epithelial cells. Scale bar (black) = 20 µm. **D,** H&E staining of patient samples shown in Fig. 1F. Scale bars (white) = 100 µm. **E,** Enrichment results of genes found to be co-expressed with TAOK3 in the scRNA-seq datasets highlights cadherin and S100 protein binding, plasma membrane, and cell leading edge.

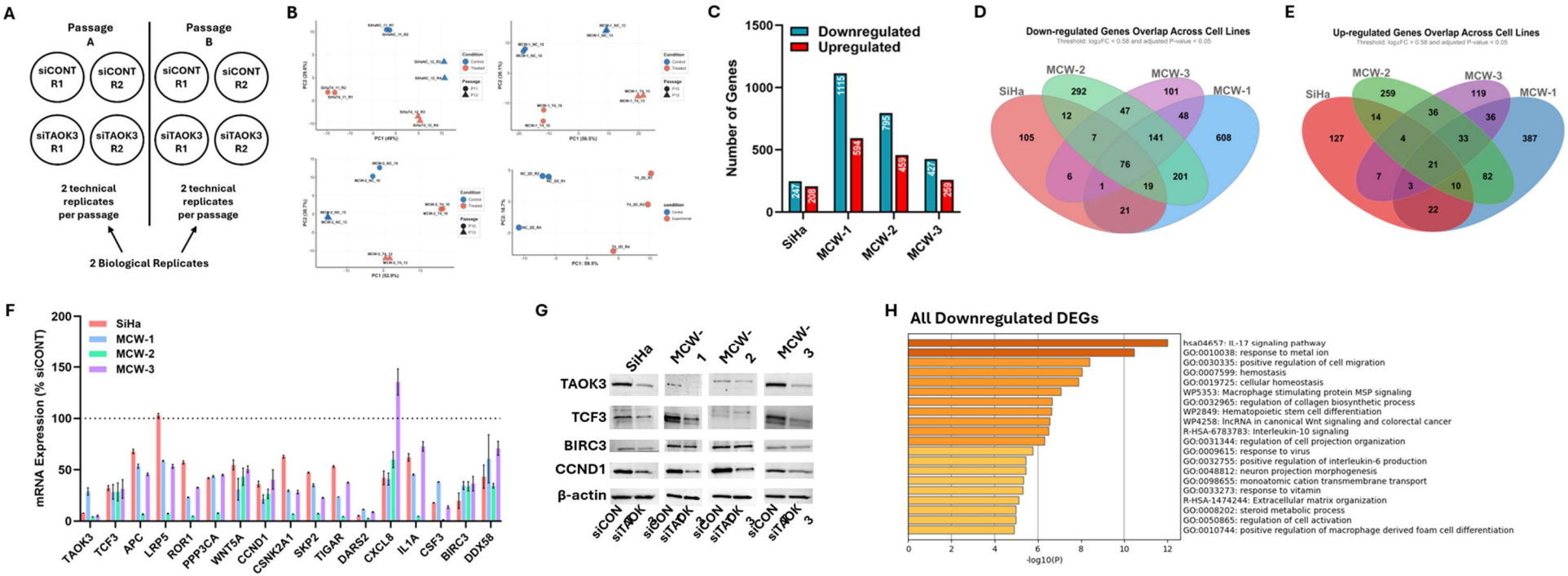

Supplementary Figure S2. Experimental design, quality control, and differential expression analysis of RNA sequencing data from *TAOK3*-silenced cervical cancer cell lines. A, Image depicting the experimental design for RNAseq samples. RNAseq was performed on *n*=8 total samples; 2 biological replicates (passages) each with 2 technical replicates (separate wells) for each passage. For the MCW-3 cell line one set of technical replicate outlier samples was removed, leaving *n*=6 total samples. **B,** PCA plots for SiHa, MCW-1, and MCW-2. **C,** Plot showing the number of downregulated (blue) and upregulated (red) DEGs found in each *TAOK3*-silenced cell line. Venn diagrams depicting the number and overlap of significantly downregulated **(D)** and upregulated **(E)** DEGs in four *TAOK3*-silenced cell lines. **F,** Quantitative PCR and **G,** western blot validation of DEG subset across four cervical cancer cell lines. **H,** Metascape ontology enrichment of all significantly downregulated DEGs (p<0.05; L2FC≤-1.0; FDR≤0.05) in *TAOK3* KD cervical cancer cell lines. **I,** Metascape ontology enrichment of all significantly upregulated DEGs (p<0.05; L2FC≥1.0; FDR≤0.05) in *TAOK3* KD cervical cancer cell lines.

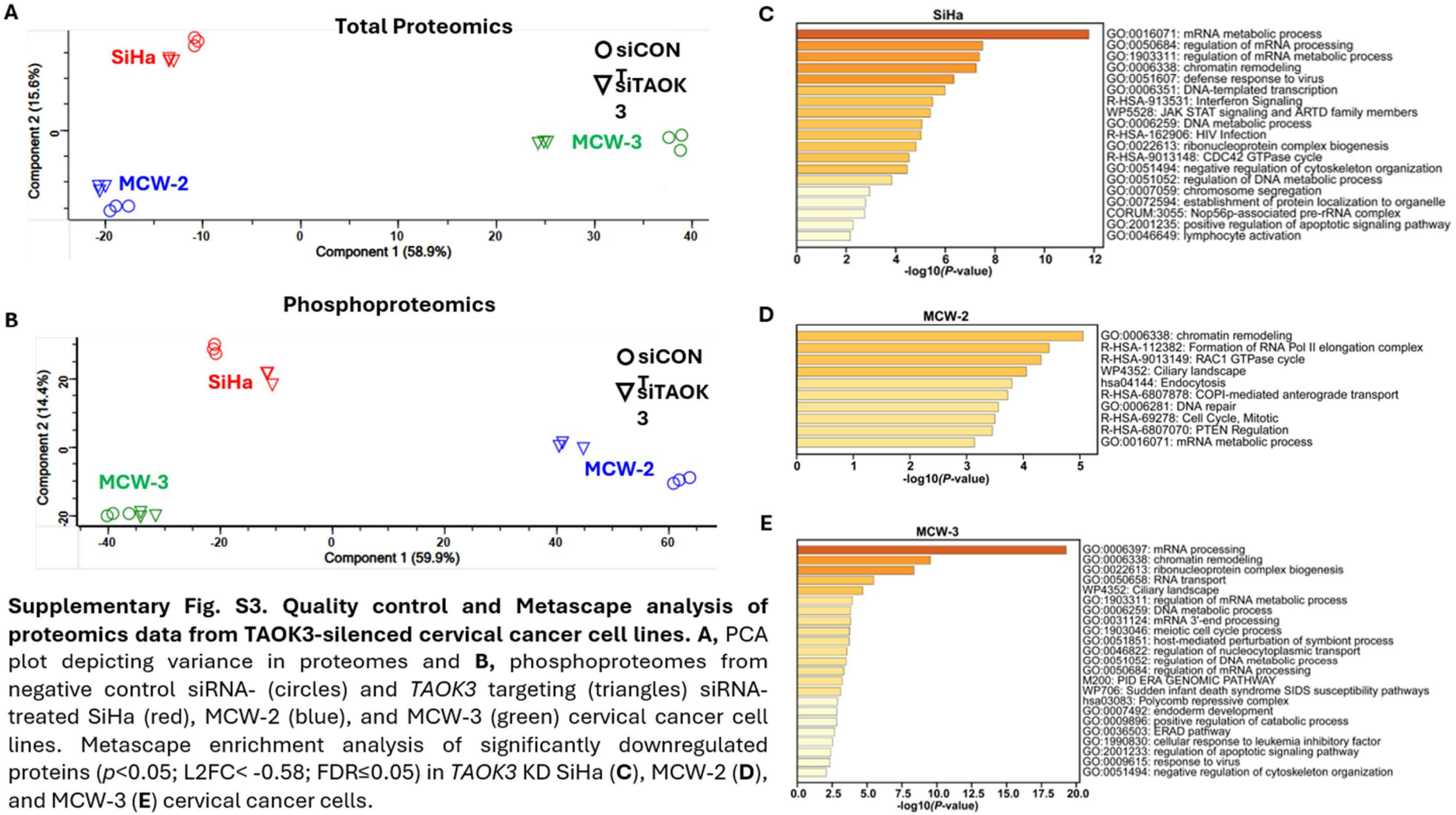

Supplementary Fig. S3. Quality control and Metascape analysis of proteomics data from TAOK3-silenced cervical cancer cell lines. A, PCA plot depicting variance in proteomes and **B,** phosphoproteomes from negative control siRNA- (circles) and *TAOK3* targeting (triangles) siRNA-treated SiHa (red), MCW-2 (blue), and MCW-3 (green) cervical cancer cell lines. Metascape enrichment analysis of significantly downregulated proteins (p<0.05; L2FC< -0.58; FDR≤0.05) in *TAOK3* KD SiHa (**C**), MCW-2 (**D**), and MCW-3 (**E**) cervical cancer cells.

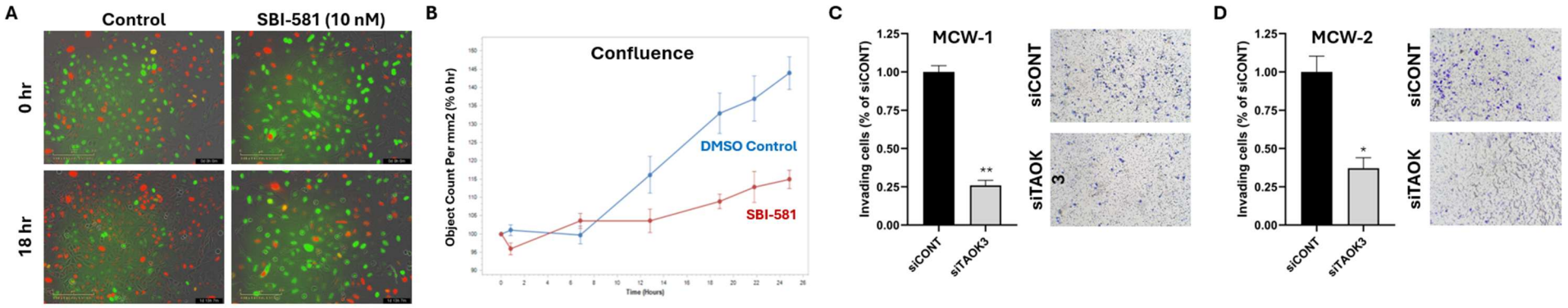

Supplementary Fig. S4. *TAOK3* inhibition affects cell cycle, invasion, and chemoresponse *in vitro*. A, Example images of Incu-SiHa cells 0 or 18 hr following double-thymidine block to investigate role of TAOK3 inhibition on cell cycle. Red = G1 phase; Green = G2M phase. **B,** Confluence analysis of Incu-SiHa cells shows significant slowing of growth in the SBI-581-treated cells (red) compared to control-treated cells (blue). **C,** TAOK3 KD in MCW-1 and **D,** MCW-2 cells resulted in significant inhibition of Matrigel invasion. *$p<0.05$; **$p<0.01$.

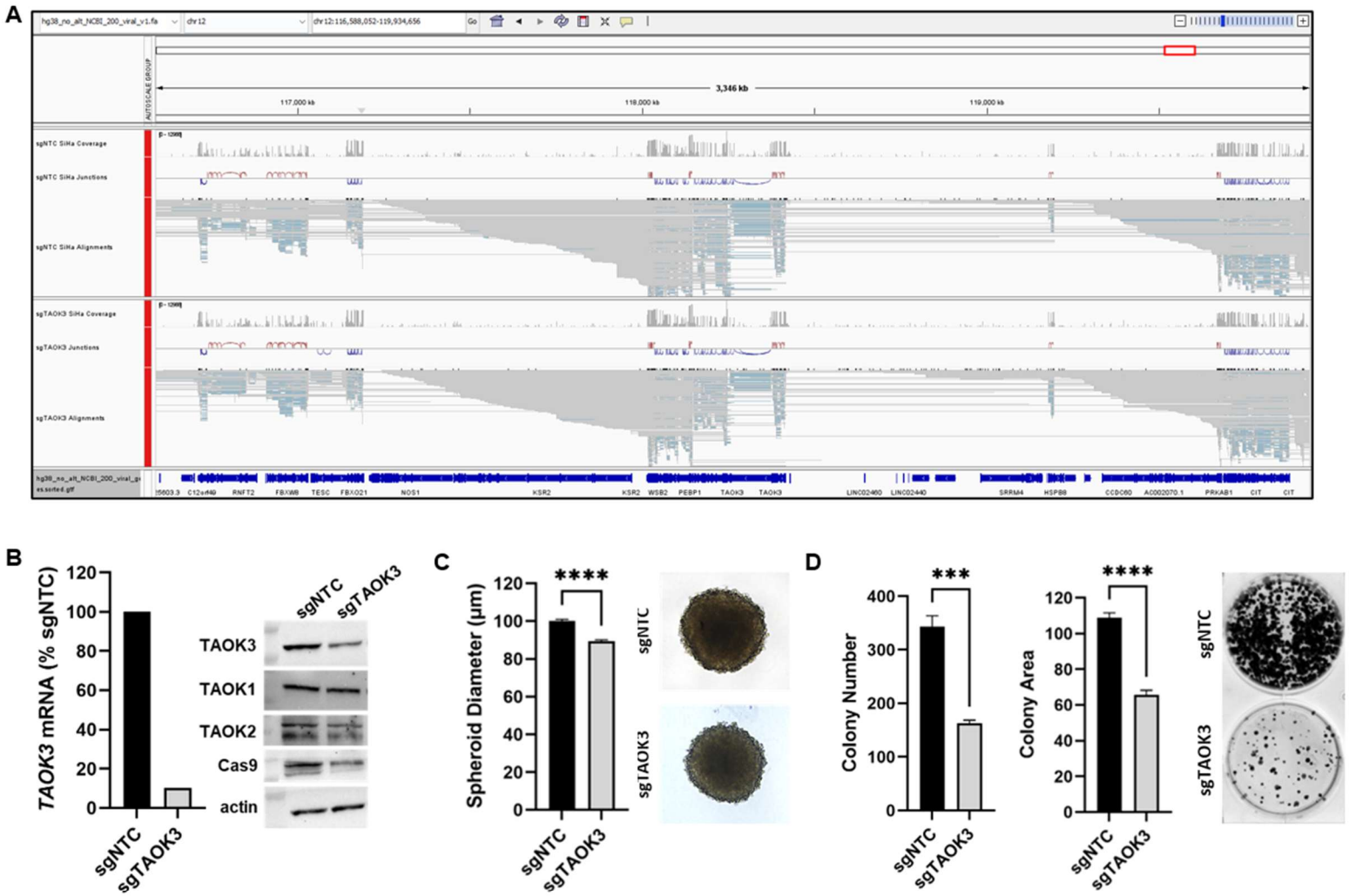

Supplementary Fig. S5. Specificity of CRISPRi-mediated *TAOK3* knockdown and effects on *in vitro* cervical cancer cell growth. A, Integrative Genomics Viewer (IGV) image showing transcriptional landscape surrounding *TAOK3* in sgNTC (top panel) and sgTAOK3 (bottom panel). **B,** *TAOK3* mRNA (left) and protein (right) were significantly downregulated in CRISPRi sgTAOK3 SiHa vs. sgNTC SiHa. **C,** sgTAOK3 spheroids were significantly smaller than sgNTC spheroids. **D,** CRISPRi-mediated KD of *TAOK3* in 2D culture resulted in significantly decreased colony number (left) and area (right). ***p<0.001; ****p<0.0001.

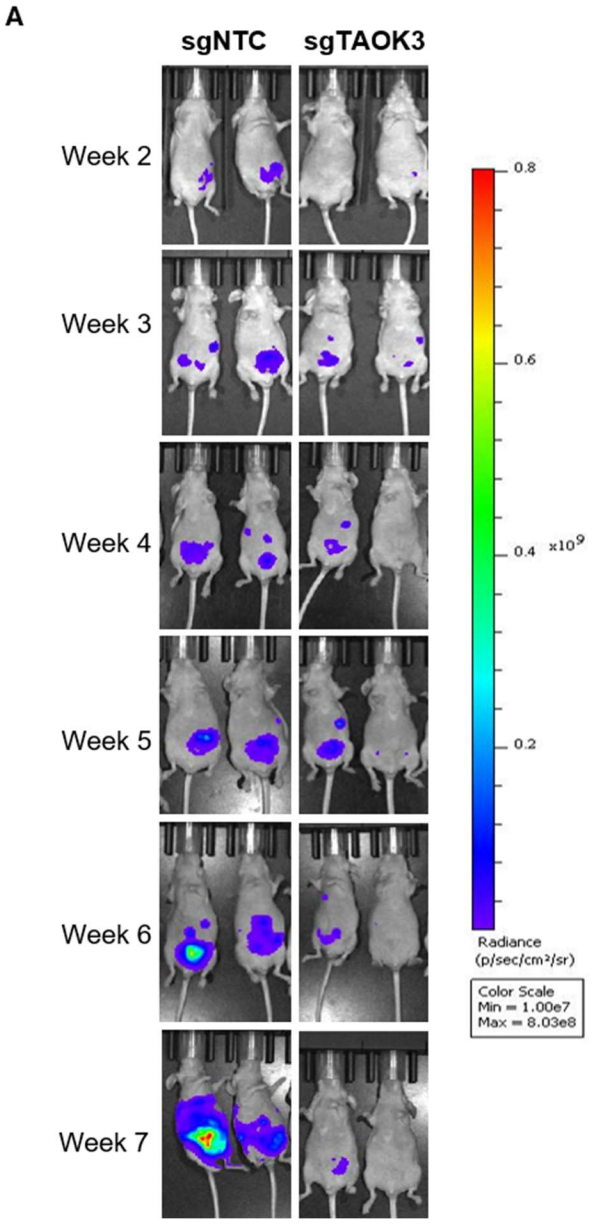

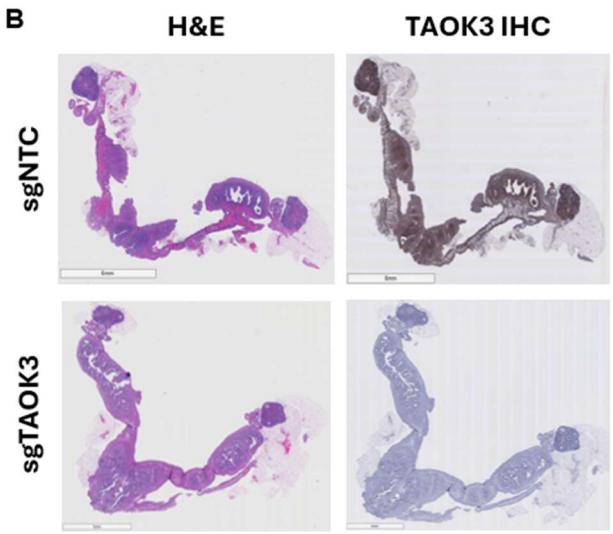

Supplementary Fig. S6. CRISPRi-mediated *TAOK3* knockdown decreases tumor burden *in vivo*. A, Example bioluminescence imaging demonstrating decreased tumor burden in sgTAOK3 mice compared to sgNTC mice. **B,** Example H&E (left panels) and TAOK3 IHC (right panels) images from sgNTC vs. sgTAOK3-injected reproductive tracts.

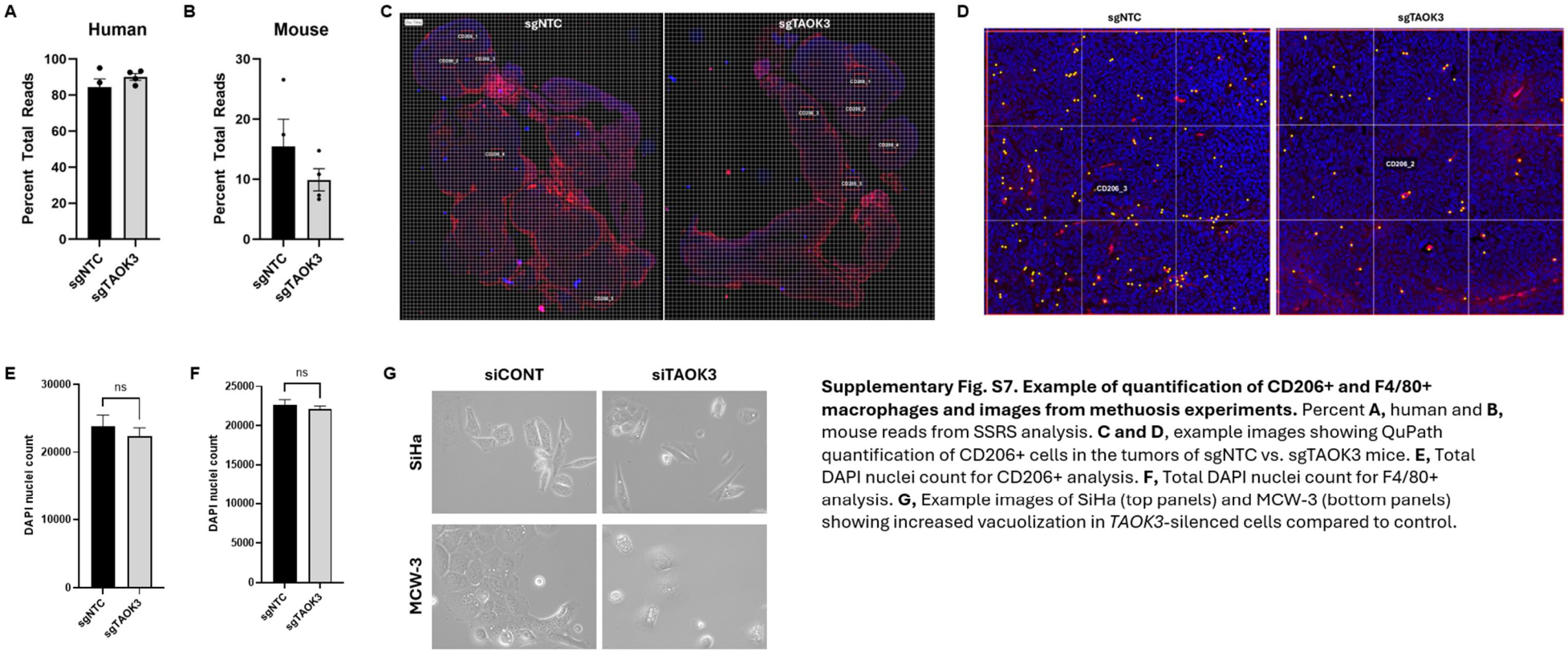

Supplementary Fig. S7. Example of quantification of CD206+ and F4/80+ macrophages and images from methuosis experiments. Percent **A,** human and **B,** mouse reads from SSRS analysis. **C and D**, example images showing QuPath quantification of CD206+ cells in the tumors of sgNTC vs. sgTAOK3 mice. **E,** Total DAPI nuclei count for CD206+ analysis. **F,** Total DAPI nuclei count for F4/80+ analysis. **G,** Example images of SiHa (top panels) and MCW-3 (bottom panels) showing increased vacuolization in *TAOK3*-silenced cells compared to control.